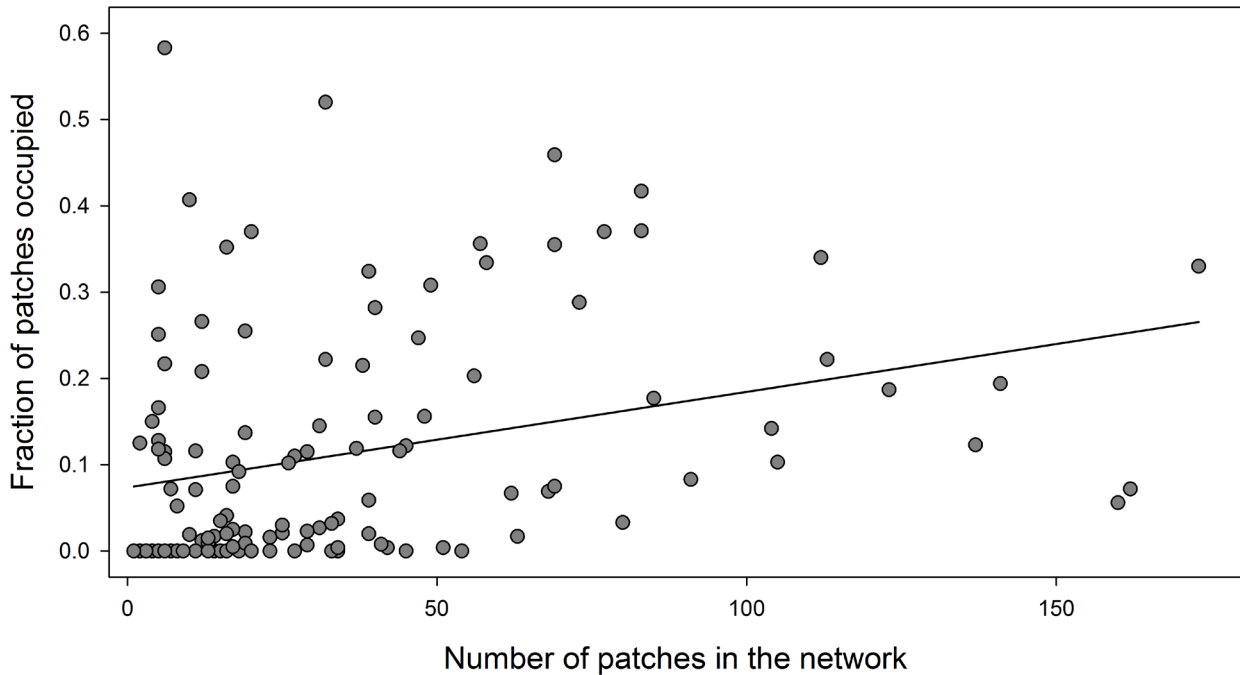
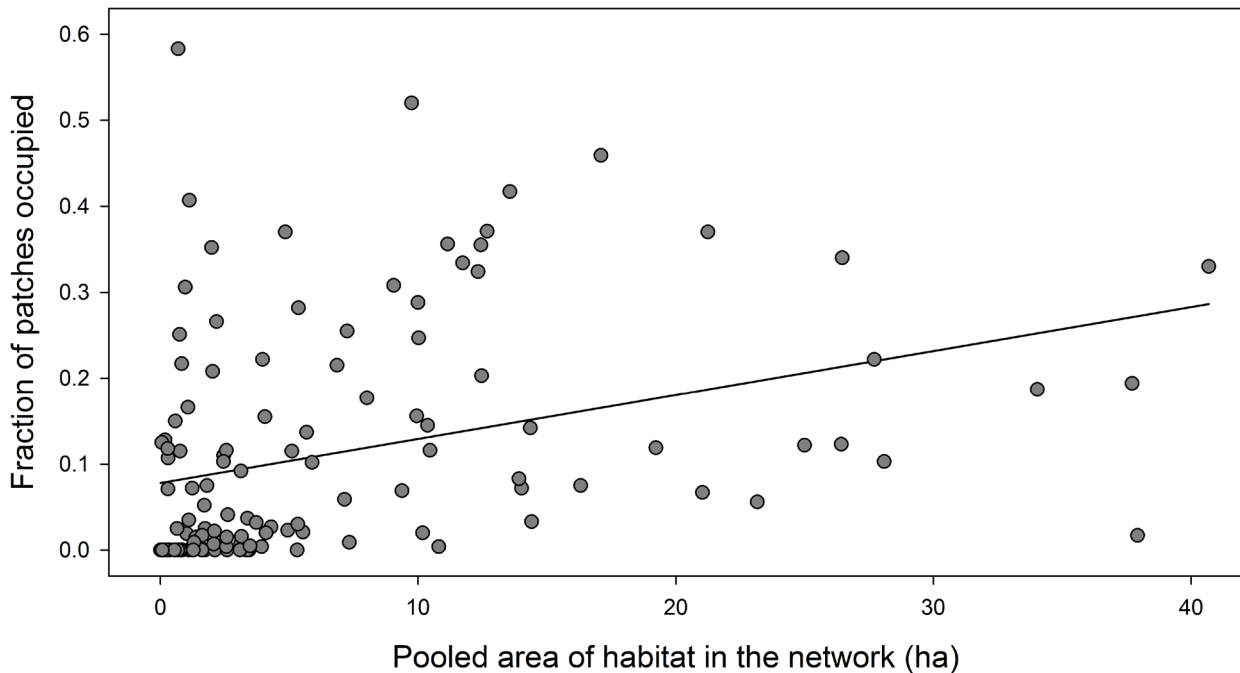


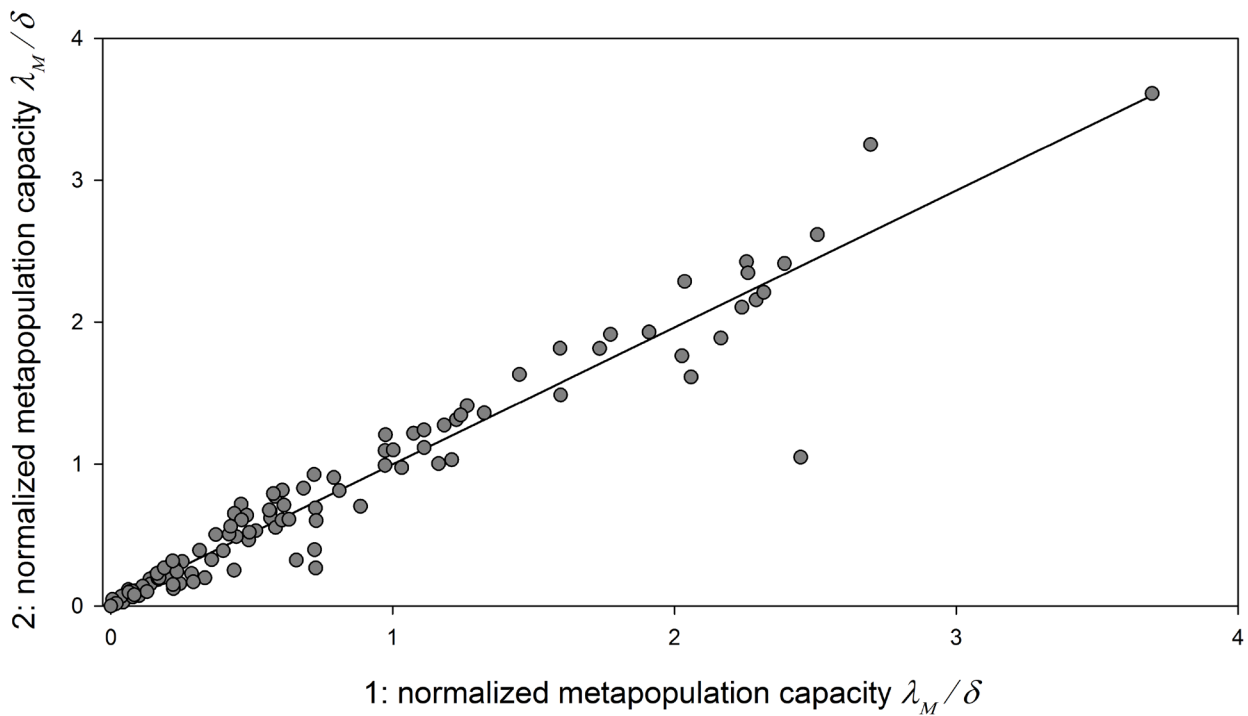
Supplementary Figures



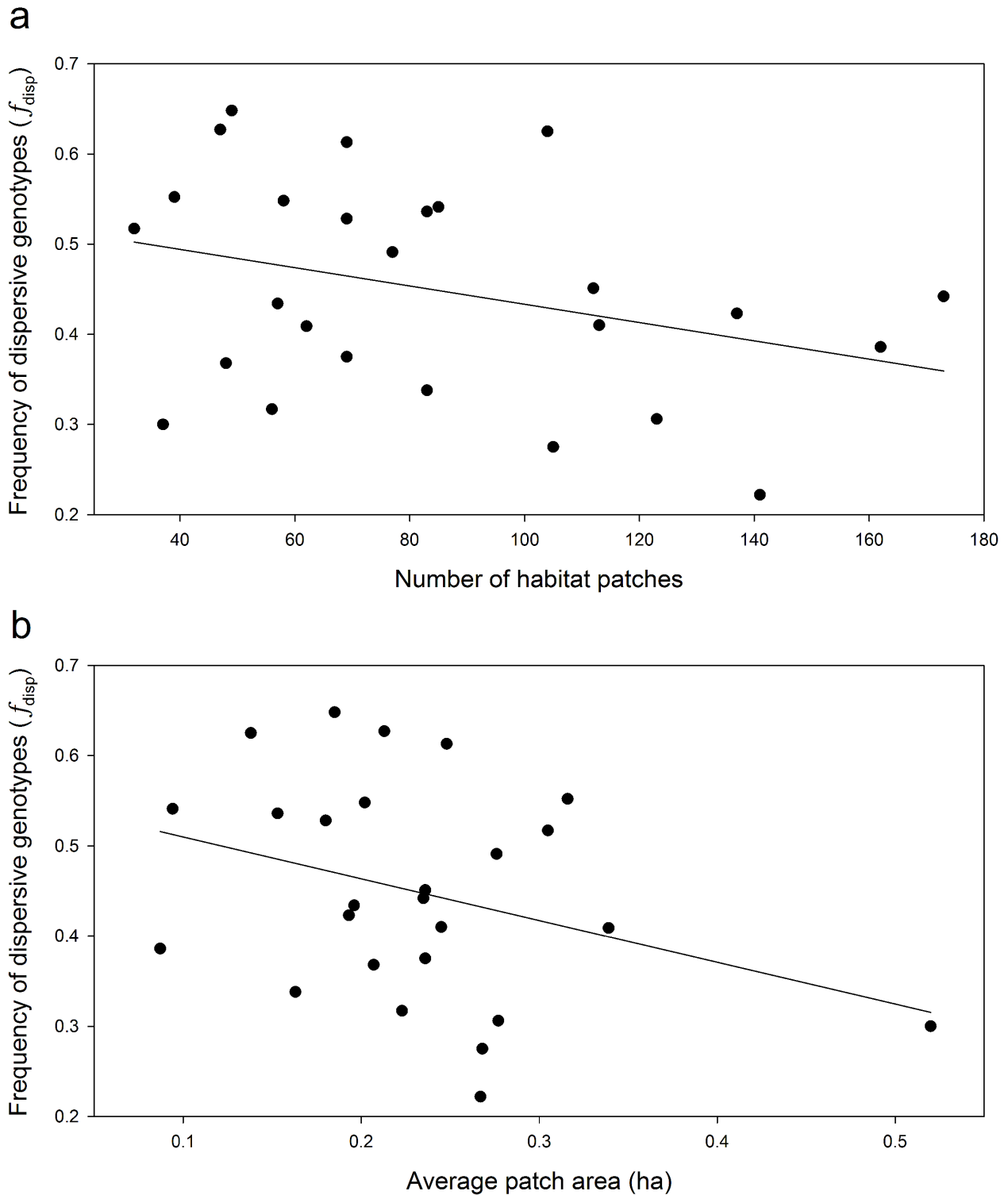
Supplementary Figure 1. Linear regression of the fraction of occupied habitat patches (p) against the number of patches in the network. The regression explains 9% of variation in p . The regression coefficient has $P = 0.0005$ (t -test: $t_{123} = 3.526$, $n = 125$).



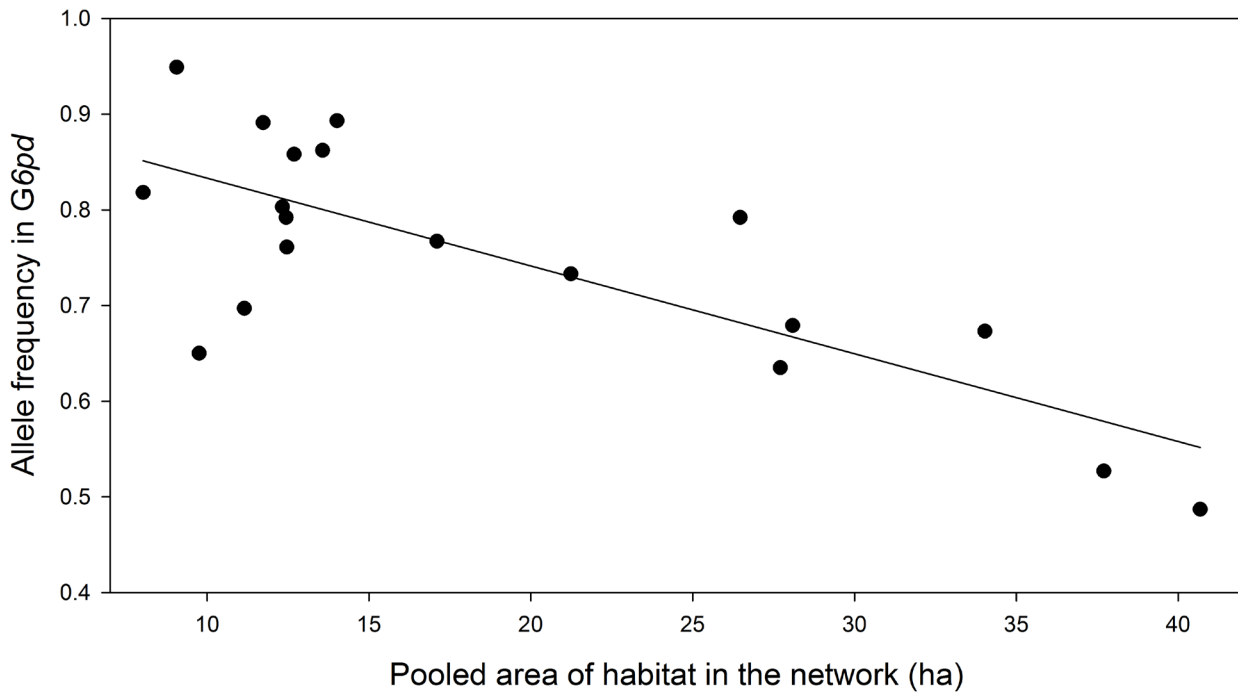
Supplementary Figure 2. Linear regression of the fraction of occupied habitat patches (p) against the pooled area of habitat in the network. The regression explains 11% of variation in p . The regression coefficient has $P = 0.0001$ (t -test: $t_{123} = 3.943$, $n = 125$).



Supplementary Figure 3. Comparison of normalized metapopulation capacities from models based on 1: annual colonization and extinction events and 2: equation (2). The metapopulation capacity λ_M estimates are normalized by dividing them by the extinction threshold parameter δ estimated in the corresponding model. In a linear regression the metapopulation capacity of model 1 explains 94 % of variation in the metapopulation capacity of model 2 (F -test: $F_{1,123} = 1969$, $P < 10^{-15}$, $n = 125$). When the metapopulation capacities are normalized, neither the intercept nor the slope of the linear regression are significantly different from zero (t -test: $t_{123} = 1.50$, $P = 0.14$, $n = 125$) and one (t -test: $t_{123} = -1.62$, $P = 0.11$, $n = 125$) respectively.



Supplementary Figure 4. Effects of the number of patches and the average patch area in the network on f_{disp} , the frequency of the dispersive genotypes in *pgi:c.331A>C*. **a**, f_{disp} decreases with increasing number of habitat patches in the network. **b**, f_{disp} decreases with increasing average size of the patches in the network. These two effects are not significant on their own, but they are both significant (F -test: $F_{2,23} = 5.969$, $P = 0.01$, $n = 26$) in a multiple regression model, which explains 28% of variation in f_{disp} .



Supplementary Figure 5. Effect of the pooled area of habitat in the network on allele frequency in a SNP Mc1:470:37074 in the gene *G6pd*. The pooled area of habitat explains 57% of variation in allele frequency. Just like in the case of the SNP *pgi*:c.331A>C, the effect of the pooled area of habitat is due to the number of patches and the average patch area in the network, which both have significant effects on allele frequency and together explain variation in allele frequency as well as the pooled area of habitat (F -test: $F_{1,17} = 24.83$, $P = 0.0001$, $n = 19$).

Supplementary Tables

Supplementary Table 1. Logistic regression model for the probability of larval group detection.

| Variable | mean | s.d. | Cr.I.-95% |
|--------------------------|-------|------|---------------|
| Intercept | -0.03 | 0.20 | -0.42 – 0.36 |
| log (Area) | -0.36 | 0.06 | -0.49 – -0.25 |
| log (Larval group count) | 0.34 | 0.07 | 0.21 – 0.41 |

The mean, standard deviation and 95% credible intervals are reported on the logit-scale. Larval group detection probabilities decrease with patch area and increase with total larval group count ($n = 200$).

Supplementary Table 2. Logistic regression model for non-detection of occupied patches.

| Variable | mean | s.d. | Cr.I.-95% |
|--------------------------|-------|------|---------------|
| Intercept | -0.48 | 0.49 | -1.42 – 0.46 |
| log (Area) | 0.25 | 0.18 | -0.09 – 0.60 |
| log (Larval group count) | -0.92 | 0.27 | -1.46 – -0.44 |

The mean, standard deviation and 95% credible intervals are reported on the logit-scale. The probability of not detecting a patch as occupied rapidly decreases with increasing population size, while patch area shows no consistent effect ($n = 200$).

Supplementary Table 3. Poisson regression model for the effect of non-detection on population size.

| Variable | mean | s.d. | Cr.I.-95% |
|----------------------------|-------|------|---------------|
| Intercept | 2.69 | 0.03 | 2.64 – 2.75 |
| log (Area) | 0.62 | 0.02 | 0.58 – 0.66 |
| Non-detection | -1.22 | 0.14 | -1.52 – -0.95 |
| log (Area) X Non-detection | -0.26 | 0.09 | -0.43 – -0.10 |

The mean, standard deviation and 95% credible intervals are reported on the log-scale. The population sizes of occupied patches are strongly determined by patch area. The population sizes of patches that were not detected during initial surveys are significantly smaller than those of detected patches of similar size, and the difference in population size between detected and non-detected populations increases with increasing patch size ($n = 200$).

Supplementary Table 4. Linear regression model for metapopulation size (\hat{p}_λ) in networks below the extinction threshold ($\delta = 5.47$).

| Variable | estimate | s.e. | t_{89} | P |
|-------------------------|----------|-------|----------|-------|
| Constant | 0.03 | 0.031 | 0.92 | 0.358 |
| Network connectivity | 0.01 | 0.003 | 3.13 | 0.002 |
| Metapopulation capacity | 0.04 | 0.012 | 3.36 | 0.001 |

The explanatory variables are network connectivity and metapopulation capacity. The model explains 17% of variation in \hat{p}_λ among the networks (F -test: $F_{2,89} = 10.56$, $P = 0.001$, $n = 92$).

Supplementary Table 5. Information on the 19 SNPs analyzed in this study.

| SNP ID | Number of networks | Number of samples | Chromosome | Scaffold | Position | Gene ID | Protein description |
|-----------------------------|--------------------|-------------------|------------|--------------|----------|---------------|---|
| Mc1:1064:194473 | 23 | 6864 | 2 | scaffold1064 | 194473 | MCINX000218 | Trypsin-like protease |
| Mc1:1353:15434 | 19 | 6368 | 15 | scaffold1353 | 15434 | MCINX001487 | Troponin-T |
| Mc1:1364:19131 | 23 | 6399 | 18 | scaffold1364 | 19131 | MCINX001528 | Hemolymph proteinase 5 |
| Mc1:1524:25351 | 19 | 6271 | 31 | scaffold1524 | 25351 | MCINX002265 | Leucyl aminopeptidase |
| Mc1:1621:69548 | 23 | 6894 | 11 | scaffold1621 | 69548 | MCINX002853 | Endocuticle structural glycoprotein SgAbd-8 |
| Mc1:1687:14486 | 21 | 6562 | 1 | scaffold1687 | 14486 | MCINX003215 | Flightin |
| Mc1:1785:58421 | 19 | 6456 | 10 | scaffold1785 | 58421 | MCINX003735 | Heat shock cognate protein 70 |
| Mc1:1791:57299 | 18 | 6162 | 1 | scaffold1791 | 57299 | MCINX003812 | Alpha-tubulin N-acetyltransferase |
| Mc1:1884:92472 | 18 | 5710 | 1 | scaffold1884 | 92472 | MCINX004366 | Triosephosphate isomerase |
| Mc1:2404:32920 | 18 | 6117 | 1 | scaffold2404 | 32920 | MCINX006747 | OCIA domain-containing protein 1 |
| Mc1:2760:8235 | 23 | 6883 | | scaffold2760 | 8235 | MCINX008073 | Vitellin-degrading protease precursor |
| Mc1:31:114406 | 18 | 6012 | 1 | scaffold31 | 114406 | MCINX009142 | Stretchin-Mlck |
| Mc1:3283:19949 pgi:c.331A>C | 27 | 7068 | 25 | scaffold3283 | 19949 | MCINX009374 | Glucose-6-phosphate isomerase |
| Mc1:337:97709 | 23 | 6885 | 22 | scaffold337 | 97709 | MCINX009609 | Prophenoloxidase-activating proteinase-3 |
| Mc1:3568:15483 | 18 | 6118 | 1 | scaffold3568 | 15483 | MCINX009942 | Leucyl aminopeptidase-like protein |
| Mc1:4593:27912 | 19 | 6403 | | scaffold4593 | 27912 | MCINX011658 | Cytochrome P450 337 |
| Mc1:470:37074 | 19 | 6244 | 2 | scaffold470 | 37074 | no gene model | Glucose-6-phosphate 1-dehydrogenase |
| Mc1:6658:103082 | 23 | 6832 | 11 | scaffold6658 | 103082 | MCINX014139 | Serpin 1 |
| Mc1:7849:5756 | 23 | 6835 | 7 | scaffold7849 | 5756 | MCINX015187 | Chymotrypsinogen-like protein |

The columns give the ID of the SNP, the number of networks above the extinction threshold for which a sufficient sample was available (>10 larval family groups), total number of individuals genotyped, the chromosome, the scaffold ID, position of the SNP in the scaffold, the ID of the gene model, and the description of the protein.